NEAR-OPTIMAL FEEDBACK CONTROL FOR THREE-DIMENSIONAL INTERCEPTIONS

J. Shinar*
Technion - Israel Institute of Technology
Haifa, Israel.

ICAS-86-5.1.3

K.H. Well**
DFVLR
Oberpfaffenhofen, FRG

and

B. Järmark***
SAAB-SCANIA AB
Linköping, Sweden.

Abstract

The paper presents two feedback approximation methods for the optimal control of an interceptor aircraft in a medium-range scenario. One method is an advanced application of forced singular perturbation techniques, while the other is an updated version of a first-order differential dynamic programming algorithm. The feedback approximations are compared to the exact open-loop optimal control solution obtained by a multiple shooting algorithm. The comparison shows that the accuracy of both feedback approximations is very satisfactory. The results emphasize the attractiveness of the feedback algorithms for airborne implementation.

I. Introduction

In the last years several feedback algorithms were developed to approximate the optimal control strategies in different types of aircraft maneuvers[1-12]. The motivation behind this effort has been the need for real-time optimized aircraft control in critical missions, particularly in air combat. The task of air-to-air interception has received great attention[4-12] for obvious reasons. One of the feedback algorithms, dealing with the point capture of a low-flying target[7], was validated in a pilot-in-the-loop simulation[13] and flight tested recently[14]. These activities have provided the encouraging proof of feasibility for such algorithms. Not only the real-time computational aspect, but more importantly the integration of the guidance commands with the aircraft display and flight control system was demonstrated.

The other consideration in evaluating the usefulness of a near-optimal feedback algorithm, as of any other type of approximation, is its accuracy in comparison to the exact optimal control solution. The investigation effort in this direction has been unfortunately very limited[10,11,15] for various reasons. In any case, the facts are that the level of accuracy and consequently the domain of practical validity of the already flight tested feedback algorithm[7,14] is still unknown.

The objective of the present paper, based on a joint effort, - the result of voluntary international scientific cooperation, - is a step towards the accuracy assessments of feedback control approximations, which are candidates for airborne implementation. The present investigation deals, as many others[4-12], with a time-optimal interception of another aircraft. The target is assumed to be detected beyond visual range and the interceptor is equipped with guided air-to-air missiles.

The paper presents two different feedback approximations: One is based on an advanced application of forced singular perturbation techniques (FSPT)[11,12] and the other is an updating version of a first-order differential dynamic (DDP) algorithm[16]. Results are compared to the exact open-loop optimal control solution obtained by a highly accurate multiple-shooting algorithm (MSA).

In section II the interception problem is formulated and the necessary conditions of control optimality are derived. A brief description of the MSA optimization technique is given in section III. Section IV presents the most recent version of an explicit FSPT feedback algorithm while the DDP updating approach is explained in section V. The numerical examples of the comparison are given in section VI and discussed subsequently.

II. Problem Formulation

Mathematical Model

The air-to-air interception analyzed in this paper has the following characteristics:

a. The target airplane flies in a fixed altitude and direction at a constant speed.

b. The initial distance of separation is

---

* Professor, Dept. of Aeronautical Engineering.
** Research Scientist, Flight Systems Dynamics Lab.
***Research Scientist, Aircraft Division.

large compared to the turning radius of the interceptor, but not large enough for allowing to reach the interceptor's maximum speed. This statement defines the domain of "medium-range" interceptions.

c. The interception terminates when the distance of separation is reduced to a prescribed value "d", determined by firing and envelope of the interceptor's weapon system.

The cartesian coordinate system used for the analysis is centered at the target airplane, the "x" axis being aligned with its velocity vector. In these axes the equations of relative trajectory are expressed by

$$\dot{x}=V\cos\gamma\cos\chi - V_e \quad ; \quad x(0)=x_0 \tag{1}$$

$$\dot{y}=V\cos\gamma\cos\chi \quad ; \quad y(0)=y_0 \tag{2}$$

$$\Delta\dot{h}=\dot{h}=V\sin\gamma \quad ; \Delta h(0)=h(0)-h_e=\Delta h_0 \tag{3}$$

The dynamics of the interceptor are described, assuming flat, nonrotating earth, point-mass approximation and thrust aligned with velocity, by the following equations of motion:

$$\dot{V} = g[(T-D)/W - \sin\gamma] \quad ; \quad V(0)=V_0 \tag{4}$$

$$\dot{\gamma} = (g/V)[(L/W)\cos\mu-\cos\gamma] \quad ; \quad \gamma(0)=\gamma_0 \tag{5}$$

$$\dot{\chi} = (g/V\cos\gamma)[(L/W)\sin\mu] \quad ; \quad \chi(0)=\chi_0 \tag{6}$$

The aerodynamic forces (lift and drag) and the maximum available thrust are functions of speed and altitude

$$L = 0.5\rho(h)V^2SC_L \tag{7}$$

$$D = 0.5\rho(h)V^2SC_L \tag{8}$$

$$T = \eta T_{max}(h,V) \tag{9}$$

The drag coefficient assumed to be a function of the Mach number and depending on the lift coefficient by a parabolic polar

$$C_D(M,C_L) = C_{D_0}(M) + K(M)C_L^2 \tag{10}$$

Using the definition of the aerodynamic load factor

$$n \triangleq (L/W) \tag{11}$$

The drag force can be expressed as

$$D = D_0 + n^2D_I = D(h,V,n) \tag{12}$$

where D_0 is the zero lift drag

$$D_0 = 0.5\rho(h)V^2SC_{D_0} \tag{13}$$

and D_I is the induced drag in level flight (n=1)

$$D_I = 2KW^2/(\rho V^2S) \tag{14}$$

The controls of the airplane in this model are:

(i) The throttle parameter η constrained by

$$0 \leq \eta \leq 1 \tag{15}$$

(ii) The bank angle "μ" which determines the direction of the lift force.

(iii) The aerodynamic load factor "n" which is subject to two different types of constraints: a structural limit which becomes active only for high velocities

$$n \leq n_{max} \tag{16}$$

and the limit imposed by the maximum usable lift coefficient, which is itself Mach number dependent,

$$n \leq n_L(h,M) \triangleq 0.5\rho(h)V^2SC_{L_{max}}(M)/W \tag{17}$$

The interception has to take place, as any other aircraft maneuver, in the flight envelope of the airplane constrained by the following:

a. minimum altitude limit

$$h \geq h_{min} > 0 \tag{18}$$

b. maximum speed limit, determined either by the maximum allowed dynamic pressure q_{max} or the maximum Mach number

$$V \leq \min\{[2q_{max}/\rho(h)]^{1/2}; a(h)M_{max}\} \tag{19}$$

c. a combined boundary of maximum altitude and minimum speed, called the "loft-ceiling" limit and defined by

$$0.5\rho(h)V^2C_{L_{max}} \geq (W/S) \tag{20}$$

Optimal Control Problem Formulation

The optimal control problem to be solved is to determine the control functions, η^*, μ^*, n^* that bring the interceptor airplane from a given set of initial conditions $(x_0, y_0, \Delta h_0, V_0, \gamma_0, \chi_0)$ to a relative final position determined by the "firing envelope" of its weapon system:

$$x_f^2 + y_f^2 + \Delta h_f^2 \leq d \tag{21}$$

in minimum time, i.e.,

$$J^* = \min_{\mu,n,\eta} J = \min_{\mu,n,\eta} t_f \tag{22}$$

The variational Hamiltonian of the problem, using (11) and (12) is

$$H = -1+\lambda_x(V\cos\gamma\cos\chi - V_e)+\lambda_y V\cos\gamma\sin\chi +$$
$$+\lambda_h V\sin\gamma+\lambda_V(g/W)(\eta T_{max}-D_0-n^2D_i-W\sin\gamma)+$$
$$+\lambda_\gamma(g/V)(n\cos\mu-\cos\gamma)+\lambda_\chi(g/V\cos\gamma)n\sin\mu+$$
$$-\vartheta_L[n_L(h,V)-n]+\text{other constraints} \tag{23}$$

The necessary conditions of optimality include differential equations

$$\dot\lambda_x = -\frac{\partial H}{\partial x} = \dot\lambda_y = -\frac{\partial H}{\partial y} = 0 \tag{24}$$

$$\dot\lambda_h = -\frac{\partial H}{\partial h} =$$
$$= -\lambda_V\frac{g}{W}\frac{\partial}{\partial h}(T-D)-\vartheta_L\frac{\partial n_L}{\partial h} \tag{25}$$

$$\dot\lambda_V = -\frac{\partial H}{\partial V} = -\left\{\lambda_x\cos\gamma\cos\chi+\lambda_y\cos\gamma\sin\chi +\right.$$
$$\left.+\lambda_h\sin\gamma+\frac{\lambda_V g}{W}\frac{\partial}{\partial V}(T-D)+\vartheta_L\frac{\partial n_L}{\partial V}\right\} -$$
$$-\frac{g}{V^2}\left\{\lambda_\gamma(n\cos\mu-\cos\gamma)+\lambda_\chi n\frac{\sin\mu}{\cos\gamma}\right\} \tag{26}$$

$$\dot\lambda_\gamma = -\frac{\partial H}{\partial\gamma} = -V(\lambda_x\sin\gamma\cos\chi+\lambda_y\sin\gamma\sin\chi$$
$$-\lambda_h\cos\gamma)+\lambda_V g\cos\gamma-\frac{g\sin\gamma}{V}\left\{\lambda_\gamma+\frac{\lambda_\chi\sin\mu}{\cos^2\gamma}\right\} \tag{27}$$

$$\dot\lambda_\chi = -\frac{\partial H}{\partial\chi} = V(\lambda_x\cos\gamma\sin\chi-\lambda_y\cos\gamma\cos\chi) \tag{28}$$

The terminal conditions of the adjoint variables are determined by the transversality conditions. Since the final time is unkown

$$H(t_f) = 0 \tag{29}$$

which leads to the following results

$$\lambda_{x_f} = \cos\theta_f\cos\Psi_f/[-\dot R(t_f)] \tag{30}$$

$$\lambda_{y_f} = \cos\theta_f\sin\Psi_f/[-\dot R(t_f)] \tag{31}$$

$$\lambda_{h_f} = \sin\theta_f/[-\dot R(t_f)] \tag{32}$$

$$\lambda_{V_f} = 0 \tag{33}$$

$$\lambda_{\gamma_f} = 0 \tag{34}$$

$$\lambda_{\chi_f} = 0 \tag{35}$$

where Ψ_f and θ_f are the final line of sight angles and $\dot R(t_f)$ is the final closing speed given by

$$\dot R(t_f) = V_e\cos\theta_f\cos\Psi_f -$$
$$-V_f[\cos\theta_f\cos\gamma_f\cos(\chi_f-\Psi_f)+\sin\theta_f\sin\gamma_f] \tag{36}$$

The optimal control functions which have to maximize the Hamiltonian, are determined by

$$\eta^* = 1/2[1+\text{sign}\lambda_V] \quad ; \quad \lambda_V \neq 0 \tag{37}$$

$$\text{tg}\mu^* = \lambda_\chi/\lambda_\gamma\cos\gamma \tag{38}$$

$$n_u^* = \Lambda\, W/2\lambda_V\cos\gamma\, D_I \tag{39}$$

where

$$\Lambda = \left\{\lambda_\chi^2+\lambda_\gamma^2\cos_\gamma^2\right\}^{1/2} \tag{40}$$

Eq. (39) is valid only if the constraints of the load factor (16) and (17) are not violated. Otherwise

$$n^* = \min[n_u^*, n_{max}, n_L(h,M)] \tag{41}$$

If the load factor is determined by (17), i.e., $n^*=n_L$

$$\vartheta_L = \frac{g}{V}\left\{\lambda_\gamma\cos\mu+\lambda_\mu\frac{\sin\mu}{\cos\gamma}-2n_L\lambda_V\frac{VD_i}{W}\right\} \tag{42}$$

Moreover, since time is not explicity involved

$$\frac{\partial H^*}{\partial t} = 0 \tag{43}$$

which leads, combined with (29) to

$$H^* = H(\eta^*,\mu^*,n^*) = 0 \tag{44}$$

The optimal control problem to be solved consists of a nonlinear two-point-boundary-value problem (NLTPBVP) determined by the set of 12 different equations (1)-(6) and (24)-(28) with the respective boundary conditions.

The natural way for obtaining the exact solution for such a problem is by some iterative algorithm which provides, assuming proper convergence, an open-loop control. For any specified set of initial conditions the optimal control variables are given as a function of time. A new set of initial conditions requires a new solution. All numerical optimization algorithms require a considerable amount of computation. For real-time onboard applications reasonably accurate sub-optimal feedback control laws are preferred. In

the present paper two such closed-loop control algorithms are outlined. Their accuracy is evaluated in comparison with a complex but very accurate optimization method explained briefly in the next section.

III. Multiple Shooting Algorithm

The theoretical basis of this numerical optimization method is described in detail in Ref. 17 and its implementation is summarized in a recent report[18]. Here only a very brief recapitulation of the method is given. The multiple shooting algorithm (MSA) solves boundary-value problems of the form

$$\dot{z} = f(z,t) \tag{45}$$

$$r[z(0),\ z(t_f)] = 0 \tag{46}$$

where z(t) is the n-vector of the dependent variables (state and multipliers), and r the n-vector of initial and final conditions on z. The basic idea of the MSA is to solve the two-point boundary-value problem by solving a sequence of initial-value problems. To this end the interval is divided by introducing the grid points

$$0 = t_1 < t_2 < \ldots < t_m = t_f$$

resulting in m-1 subintervals. In each subinterval $t\in[t_j,t_{j+1}]$, j=1, ...,m-1 the initial-value problem

$$\dot{z} = f(z,t) \tag{47}$$

is solved with the initial conditions

$$z(t_j) = Z_j \tag{48}$$

Starting with an initial guess $Z_j^{(o)}$, j=1,...,m-1, the problem then consists of finding values for Z_j such that the solutions are continuous across the subintervals and the boundary conditions are satisfied. In other words, the function

$$\lambda = (\lambda_1,\lambda_2,\ldots,\lambda_{m-1})^T \tag{49}$$

$$\lambda_j = z(t_{j+1},Z_j) - Z_{j+1},\ j=1,\ldots,m-2 \tag{50}$$

$$\lambda_{m-1} = r[Z_1, z(t_m,Z_{m-1})] \tag{51}$$

must vanish. The components of λ are the jumps across the grid points. Applying the Newton method for adjusting the Z_j the linear system

$$\begin{bmatrix} G_1-I & & & \\ & G_2-I & 0 & \\ & & \ddots & \\ & & & G_{m-2}-I \\ A & & & BG_{m-1} \end{bmatrix} \begin{bmatrix} \Delta Z_1 \\ \Delta Z_2 \\ \vdots \\ \Delta Z_{m-2} \\ \Delta Z_{m-1} \end{bmatrix} = - \begin{bmatrix} \lambda_1 \\ \lambda_2 \\ \vdots \\ \lambda_{m-2} \\ \lambda_{m-1} \end{bmatrix} \tag{52}$$

has to be solved for ΔZ_j with

$$G_j = \frac{\partial z(t_{j+1},Z_j)}{\partial Z_j} \tag{53}$$

$$A = \frac{\partial r}{\partial z(0)}\ ,\quad B = \frac{\partial r}{\partial z(t_f)} \tag{54}$$

and I the unit matrix. Defining

$$F = A + BG_{m-1}G_{m-2}\ldots G_1 \tag{55}$$

$$U = -\left[\lambda_{m-1} + BG_{m-1}\lambda_{m-2} + \ldots + BG_{m-1}G_{m-2}\ldots G_2\lambda_1\right] \tag{56}$$

(52) can be written formally as

$$F\Delta Z_1 = U \tag{57}$$

After solving for ΔZ_1 the other corrections are obtained recursively from

$$\Delta Z_j = \lambda_{j-1} - G_{j-1}Z_{j-1}\ ,\ j=2,\ldots,m-1 \tag{58}$$

The new values for Z_j are computed by

$$Z_j^{(k)} = Z_j^{(k-1)} + \delta DZ_j \tag{59}$$

with δ as a relaxation factor of the Newton method. The choice of δ is most important for the MSA to perform efficiently.

The MSA has been applied successfully to many trajectory optimization problems, such as in Ref. 19. The method is especially powerful in connection with "continuations", that is whenever solutions are to be expressed as functions of one or several parameters. In the present paper it is used as a reference for comparison in the accuracy assessment of two suboptimal feedback algorithms described in the subsequent sections.

IV. Advanced FSPT Guidance Law

The feedback algorithm described in this section is the latest version of a family of analytically derived explicit control laws based on the approach of forced singular perturbation. It is the three-dimensional synthesis of two improved planar interception algorithms in the horizontal[11] and the vertical[12] planes.

Applications of singular perturbation theory to aircraft performance optimization has been based on observing an actual time-scale-separation between different state variables. In simple (linear, time-invariant) dynamic system such a time-scale-separation is expressed by a small parameter ε, the ratio of the respective eigenvalues and can be made evident by a scaling transformation. The scaling transformation results in multiplying the time derivative of the "fast" variable by ε. By setting

$\varepsilon=0$ fast dynamics are neglected and the order of the dynamic system is reduced. The solution of the "reduced-order" system can serve as an approximation of the actual problem but it cannot satisfy the initial and eventual terminal conditions imposed on the "fast" variables. This deficiency is corrected by initial and terminal "boundary layer" solutions computed on a stretched time-scale ($\tau=t/\varepsilon$). Thus the solution of a singularly perturbed dynamic problem consists of the "reduced-order" solution with asymptotically matched "boundary layer" solutions. In the "reduced-order" solution the fast variables are considered as pseudo-controls, while in the "boundary layer" solutions the "slow" variables are kept frozen to their initial (or terminal) values.

In the strongly nonlinear problems of flight mechanics the formal identification of a small parameter, associated with the experienced time-scale-separation, can be very inconvenient. For this reason it was proposed[1] to insert the perturbation parameter ε artificially as a multiplier of the fast time-derivatives. This approach, called later[5] as "forced singular perturbation technique" (FSPT) has been adapted for aircraft performance optimization[2-12] (though not in all papers it is referred to as such).

The particular characteristics of the advanced FSPT guidance law presented here can be summarized, in comparison to the other type of feedback algorithms based on a similar approach[4,7,10], in the following points:

a. It is oriented towards a minimum-time guided missile firing rather than for point capture.

b. It expresses the optimal control law as an explicit function of the state variables and aircraft performance parameters.

c. It assumes that horizontal and vertical turning dynamics belong to the same time-scale.

d. It includes an asymptotically matched "terminal boundary layer" allowing a "zoom" trajectory for interception of high flying targets[12].

e. It can be augmented by first-order correction terms[11] if higher accuracy or enlarged domain of validity is needed.

The "reduced-order" model in this algorithm is of three state variables, x,y, and E (the specific energy) defined by

$$E = h + V^2/2g \tag{60}$$

and its rate of change (the specific power) is obtained from (3),(4),(9) and (12)

$$\dot{E} = [\eta T_{max}(h,V)-D(h,V,n)]V/W \triangleq p_s \tag{61}$$

In this formulation E replaces the speed as a state variable and V serves merely as a convenient abbreviation for

$$V = [2g(E-h)]^{1/2} \tag{62}$$

The dynamics of the reduced-order problem (where all variables are denoted by the superscript R) is composed of the differential equations (1)-(2) and (61) together with 3 algebraic constraints obtained by multiplying (3),(5) and (6) by ε (the forced singular perturbation parameter) and then setting $\varepsilon=0$. These equations yield

$$\mu^R = 0 \tag{63}$$

$$\gamma^R = 0 \tag{64}$$

$$n^R = \cos\gamma^R \tag{65}$$

The reduced order optimization problem consists of (24), an equivalent of (26) for

$$\dot{\lambda}_E = -\frac{\partial H}{\partial E}\Big|_h \tag{66}$$

and 3 algebraic equations obtained from the left had sides of the properly reformulated (25),(27) and (28) set to zero. These last equations

$$\frac{\partial H^R}{\partial h^R} = \frac{\partial H^R}{\partial \gamma^R} = \frac{\partial H^R}{\partial \chi^R} = 0 \tag{67}$$

imply that h^R,γ^R, and χ^R are to be considered as new control variables (in addition to η^R,μ^R,n^R).

The consequence of (24),as well as of (28) set to zero, together with (30) and (31) is

$$\tan\chi^R = \lambda_y^R/\lambda_x^R = \tan\psi_f \tag{68}$$

implying that χ^R=const. This leads to the conclusion that the reduced-order trajectory is confined to a fixed vertical plane and therefore results of Refs. 8 and 12 can be applied yielding

$$\eta^R = 1 \tag{69}$$

$$h^R = \arg\max_h \frac{p_s(E,h)}{V_f^R(E_f)-V^R(E,h)} = h^R(E,E_f) \tag{70}$$

Equations (69)-(70) imply a full thrust climbing acceleration towards the final speed V_f^R, the highest speed attainable at the final specific energy level E_f. This variable trajectory is certainly incompatible (physically) with (64). The actual flight path angle along every smooth part

of the trajectory is given [combining (3)-(4) and (61)]

$$\sin\gamma^R \triangleq P_s^R/V^R\left(1 + \frac{V^R}{g}\frac{dV^R}{dh^R}\right) \tag{71}$$

which replaces in the sequel the non-physical prediction of (64). The absolute value of γ^R is, however, assumed to be sufficiently small so that the approximation

$$\cos\gamma^R \approx 1 \tag{72}$$

can be used in conjunction with (65). The horizontal distance covered during the climbing acceleration is

$$\Delta s = \int_{t_o}^{t_f} V^R\cos\gamma^R dt \cong \int_{E_o}^{E_f} \frac{V^R(E)}{P_s^R(E)}\,dE \tag{73}$$

and the time associated with it is given by

$$\Delta t = \int_{t_o}^{t_f} dt = \int_{E_o}^{E_f} \frac{V^R(E)}{P_s^R(E)} \tag{74}$$

If the final point $[E_f, h^R(E_f)]$ is inside the q_{max} boundary i.e.

$$\frac{1}{2}\rho(h^R)V^{R^2} < q_{max} \tag{75}$$

then at this point by definition $P_s^R=0$, which makes the integrals in (73),(74) singular. Such singularity can be avoided by replacing (73) and (74) with

$$\Delta s' = \int_{E_o}^{E_f^*} \frac{V^R(E)}{P_s^R(E)}\,dE \triangleq I_s \tag{76}$$

$$\Delta t' = \int_{E_o}^{E_f^*} \frac{dE}{P_s^R(E)} \triangleq I_s \tag{77}$$

where $E_f^*=0.99\ E_f$. Note that (70) and consequently the entire reduced-order vertical flight path depends on the parameter V_f^R, which is a function of E_f itself. For any given initial specific energy E_o the integrals I_s and I_t are functions of E_f and can be precomputed and stored. With the stored values of $I_s(E_f)$ the solution of the three-dimensional reduced-order problem can be completed. The horizontal projection of the trajectory has to satisfy (see Fig.2)[11].

$$(I_s+d)\cos\chi^R = V_T I_t + R_o\cos\psi_o \tag{78}$$

$$(I_s+d)\sin\chi^R = R_o\sin\psi_o \tag{79}$$

where $R_o=(x_o^2+y_o^2)^{1/2}$, $\psi_o=\tan(y_o/x_o)$ and "d" is defined by (21). Simultaneous solution of (78),(79) yields both χ^R and E_f allowing to determine the appropriate altitude profile $h^R(E,E_f)$ matching the initial conditions of the interception (x_o,y_o).

Since, in general, $h_o \neq h^R(E_o)$ a "boundary layer" correction is needed. The control variable in this layer is the flight path angle expressed in a feedback form [8,12]

$$\cos\gamma^c \triangleq \frac{VP_s^R}{V^R P_s - V_f^R(P_s^R - P_s)}\,\mathrm{sign}(h^R-h) \tag{80}$$

This expression equally holds for $h=h^R(E)$, because in this case $V=V^R(E)$ and $P_s(h,v) = P_s^R(E)$ leading to $\gamma^c=0$.

If the initial orientation of the interceptor velocity vector, expressed by γ_o, χ_o, does not satisfy the "reduced-order" solution $\chi^R(x_o,y_o)\neq\chi_o, \gamma^c(h_o,E_o)\neq\gamma_o$, two initial boundary layers are needed to define the horizontal and vertical load factor components. The FSPT method leads to express these load factor components in an explicit feedback form

$$n_h = \left[\frac{2V}{V_f^R - V}\left(\frac{T_{max}-D_o}{D_I} - 1\right)\right]^{1/2}\sin\left(\frac{\chi^r-\chi}{2}\right) \tag{81}$$

$$n_v = \left\{\frac{2V^R}{V_f^R - V^R}\,\frac{T_{max}-D_o^R-D_I^R\cos^2\gamma^R}{D_I\cos\gamma^R}\right\}^{1/2}\sin\left(\frac{\gamma^R-\gamma}{2}\right) + \cos\gamma \tag{82}$$

where

$$\chi^r \triangleq \chi^R(x,y,V_e) \tag{83}$$

and

$$\gamma^r = \gamma^c(h,E) + \gamma^R(E) \tag{84}$$

The structure of (81),(82) guarantees the asymptotic behavior of both boundary layers. The total load factor and the respective bank angle are obtained from (81), (82) by

$$n = \min[(n_h^2+n_V^2)^{1/2},\ n_{max}, n_L(h,V)] \tag{85}$$

$$\mu = \tan^{-1}(n_V/n_h) \tag{86}$$

Since the solution presented here is independent of the target altitude h_e a "terminal boundary layer" is needed in the vertical projection. If $h_e<h^R(E_f)$, the solution is a line along the q_{max} constraint as shown in Ref. 7. If $h_e>h^R(E_f)$,

the final portion of the trajectory has a "zoom-climb" characteristics. A feedback approximation based on the assumptions of negligible specific energy change in this phase is developed in Ref. 12. It generates a reference trajectory, asymptotically matching the reduced-order altitude profile $h^r(E)$ and associates the required flight path angle γ^z with the line of sight elevation θ. In this terminal phase the vertical load factor n_V^z is given by

$$n^z = 2\cos\gamma + \frac{W}{2D_I}\tan[\gamma^z(\theta)-\gamma] \qquad (87)$$

replacing (82).

Eventual discontinuities of the reduced-order altitude profile, such as the "transonic jump" are smoothed by a prediction technique described also in Ref. 12.

It can thus be summarized that the FSPT algorithm provides a uniformly valid explicit feedback control law approximating the optimal solution. The reduced-order solution needs some simple iterations to solve (78),(79) at the beginning. Most of the computations are in an explicit feedback form using real-time measurements of the state variables. The few simple predictive calculations, such as in the transonic jump smoothing and in the terminal zoom matching, are to be carried out in parallel with real-time guidance law computation without interference. The same rule applies for the eventual updating of the reduced-order solution. Therefore in an airborne implementation of the FSPT guidance law no special computational effort is required

V. DDP Algorithm

Open-Loop Control

Differential dynamic programming (DDP) is one of the numerical algorithms used in solving optimal control problems[20]. It is essentially an open-loop solution which is not sensitive to errors in the problem parameters, but has some difficulties in convergence. Associated with a convergence control parameter (CCP) technique[16,21] this algorithm became an efficient computational tool. The combined DDP/CCP computational process can be described (referring to the interception formulated in the present paper) by the following steps:

1. Start by guessing proper nominal controls $n_h(t)$ and $n_V(t)$. Use these controls together with $\eta=1$ to integrate the equations of motion (1)-(6) from $t_o=0$ until (21) is satisfied. Store this nominal trajectory $[x(t),y(t),h(t),V(t),\gamma(t),\chi(t)]$ together with the nominal controls. Determine $J=t_f$ from (21) and store it.

2. Since satisfying (21) provides θ_f and γ_f, the end conditions of all adjoint variables are given. Integrate (24)-(28) backward with the respective end conditions (30)-(34) along the nominal trajectory. Define a modified Hamiltonian as

$$\bar{H} = H + 0.5[C_h(\bar{n}_h-n_h)^2 + C_V(\bar{n}_V-n_V)^2] \qquad (88)$$

where C_h and C_V are convergence control parameters.

Based on (88) compute the optimal controls

$$n_h=(C_h\bar{n}_h+g\lambda_\chi V\cos\bar{\gamma})/(C_h+2\lambda_V g\ D_I/W) \qquad (89)$$

$$n_V=(C_V\bar{n}_V+g\lambda_\gamma/\bar{V})/(C_V+2\lambda_V g\ D_I/W) \qquad (90)$$

The predicted cost change caused by using these new controls is obtained by integrating backwards

$$\dot{b}_h=g[\lambda_V(D_I/W)(\bar{n}_h+n_h)-\lambda_\chi/\bar{V}\cos\bar{\gamma}](\bar{n}_h-n_h) \qquad (91)$$

$$\dot{b}_V=g[\lambda_V(D_I/W)(\bar{n}_V+n_V)-\lambda_\gamma/\bar{V}](\bar{n}_V-n_V) \qquad (92)$$

with the end conditions $b_h(t_f)=b_V(t_f)=0$.

Store the control histories $n_h(t),n_V(t)$ and the predicted cost change

$$\Delta J = [b_h(t_o) + b_V(t_o)] \qquad (93)$$

3. Use the stored control histories $n_h(t),n_V(t)$ to integrate the state equation (1)-(6) generating a new trajectory until (21) is satisfied. Compute the new cost J. Compare the difference (J-J) with ΔJ of (93). If they are of the same order of magnitude then decrease the value of C_h,C_V and repeat step 2 until it leads to a satisfactory convergence. If the comparison is not satisfactory the values of the CCP parameters have to be increased as it is described in detail in Ref. 21.

Closed-Loop Near Optimal Control

The above described process provides in most cases a reasonable accurate open-loop solution with a small number of iterations. The idea of a near-optimal closed-loop control is based on the trade-off between computational speed and accuracy. It is well known that any fast converging open-loop control solution can be applied for the synthesis of a feedback algorithm by using only the optimal control functions computed for the initial state, because the current state can always be considered as a new (updated) initial state. Measuring the current state and using a set of fixed controls for a short period of time allows to predict the future state with high accuracy. If the control algorithm converges to a level of acceptable accuracy during the same period then in the next step this optimal control can be used. By this approach an updating closed-loop almost optimal control scheme is generated. Such

a closed-loop structure is indeed necessary for real-time control in order to correct for disturbances, uncertainties and other errors neglected in an open-loop set-up.

The first initiative to use the DDP algorithm for this purpose is to be credited to Anderson[22] in several aerospace differential game applications. In the present paper this method is applied to an air-to-air interception problem. In Ref. 23 it was found that the optimal updating period is equal to one step of a DDP iteration, which is in any case the shortest possible period. The time required to complete such an iteration is proportional to the time-to-go (t_f-t)

$$(\Delta t)_i = K_{cal}(t_f - t) \qquad (94)$$

where K_{cal} can be in the range of 0.05-0.1 for an acceptable accuracy.

Difficulties of Terminal Control

It has been observed that the combined (DDP)(CCP) algorithm may have an oscillatory behavior when the pursuer becomes near the evader. This inconvenience is treatable by increasing the CCP values but then the convergence process becomes slow and consequently unacceptable for an updating closed-loop application. This deficiency can be corrected by combining the DDP with another control law for the terminal phase of the trajectory. For a horizontal engagement[24] the FSPT straight line end phase can be used, while in a vertical plane pursuit-evasion game[25] a singular control is applied. In the present paper a different approach, based on a fictive ("dummy") target located well behind the actual target, is introduced. Since the oscillatory behavior of the convergence is mostly felt in the final line of sight angles θ_f and Ψ_f used in the transversality conditions (30)-(32) a larger dummy target range

$$R_d = R_f + (\Delta R)_d \qquad (\Delta R)_d >> R_f \qquad (95)$$

will lead to smaller variations in these variables for two subsequent iterations. Since at the terminal phase the direction of the closing velocity is very near to the line of sight, minimizing the time to reach R_d to the dummy target is equivalent to reach R_f for the actual target.

Implementation

The implementation of the near-optimal closed-loop DDP algorithm was carried out with a rather simple Euler type integration with a step size of 1 sec.

The nominal controls $\bar{n}_h, \bar{n}_V$ were obtained from two different sources. The horizontal load factor component n_h was computed by the zeroth-order FSPT algorithm (81). For the vertical projection n_V a simple climb initiated by a gradual pull-up manuever was used. The value of K_{cal} used in the updating process was set to 0.05. The initial CCP values were relatively large (C_h=10, C_V=25) in order to guarantee satisfactory convergence. The computations were performed in an ordinary size IBM PC, which by itself indicates the potential of on-line implementation.

VI. Numerical Results

In the space limited scope of the present paper two sets of interception examples were computed by the three different algorithms (MSA, FSPT, DDP/CCP) described in sections III-V. In all examples an available interceptor aerodynamic and propulsion model (an idealized version of an F4-E) was used. In this model aerodynamic coefficients are expressed as polynomials of the Mach number. The maximum thrust (with afterburner) is given in a similar polynomial form but with altitutde dependent coefficients. The general interceptor data, including the major flight envelope parameters, is presented in Table 1.

Table 1. General Interceptor Data

Combat Weight	W	= 20.000 kg
Wing Area	S	= 49.25 m^2
Maximum static thrust at sea level	T_{max_0}	= 121271 N
Limit load factor	n_{max}	= 5.0
Maximum lift coeffcient ($M \leq 0.6$)	$C_{L_{max}}$	= 1.17
Dynamic pressure limit	q_{max}	= 83850 N/M^2

The objective of the first set of examples is to evaluate the accuracy of the latest FSPT version[12] for vertical interception. In a previous paper[12] it was demonstrated that a set of improvements, introduced for the correction of errors created by identifiable sources[8], indeed shortened the interception time. However, comparison with the exact optimal solution has not yet been made, and absolute accuracy has not been assessed.

The initial conditions of the interceptor in all vertical examples are kept to be the same. Target speed and altitude varied from one example to the other, but target direction was always towards to the interceptor (χ_0=180°). The different data is summarized in Table 2.

The main objective of the second set of examples is to assess the effect of coupling between horizontal and vertical turning dynamics in a three-dimensional interception for different initial interceptor velocities as summarized in Table 3.

The end results, i.e. the interception time for a fixed terminal range $R(t_f) \triangleq d$=1km

computed by the different algorithms for the 6 examples are summarized in Table 4. These results are discussed in the following section.

Table 2. Vertical Interception Data

Initial Conditions R_o= 82.8 km, h_o= 1 km
V_o= 250 m/s, γ_o= 0° , χ_o= 180°

Target Data χ_e= 0°.

Example No.	1	2	3
h_e[km]	4.18	7.0	12.0
V_e[m/s]	300	300	400

Table 3. 3-D Interception Data

Target Data h_e= 7km , V_o= 250m/s, χ_e= 0°.

Initial Conditions R_o= 82.8km, Ψ_o= 30°.

Interceptor h_o= 1km , γ_o=0°, χ_o=180°

Example No.	4	5	6
V_o[m/s]	220	250	330

VII. Discussion of Results

Comparison of the closed-loop DDP/CCP updating to the optimal open-loop solution indicates that this algorithm leads to very satisfactory results. Based on a reasonably good nominal control the pay-off accuracy is of the order of 0.5% or better. The results are not handicapped by the crude integration, though they are very sensitive to the selected nominal control. The relatively larger error in Ex. 4 is indeed the consequence of a less successful choice of nominal control.

The assessment of the FSPT results is more complex. The pay-off of FSPT algorithms described in section IV (denoted "original" in Table 4) is of the order of 1% and in this respect it can be considered as a satisfactory approximation. However, there is a substantial difference between the optimal and suboptimal (FSPT) trajectories particularly in the subsonic region. This discrepancy is illustrated the best by comparing the flight path angle time histories for Example No. 1 in Fig. 3.

The optimal trajectory starts with a gradual pull-up from the horizontal initial condition and the maximum value of the flight path angle does not exceed 18°. The FSPT solution has an initial dive phase towards the reduced-order trajectory, obtained by the energy-state approximation, and then closely follows it with relatively high flight path angles (beyond 30°) until the transonic-jump domain is reached. At supersonic speeds (t>30sec) the differences are rather small.

This observation leads to conclude that the subsonic segment of the energy-state reduced-order solution, used in the past in many studies (Refs. 4,6-10,12) but not yet tested, is unfortunately very far from being optimal. The major reason for this nonoptimality in a interception problem is the invalid assumption of $\cos\gamma \approx 1$. If the energy-state reduced-order solution is not adequate then also the corresponding boundary layer (requiring an initial dive), is not needed. In order to eliminate the part of the error which is contributed by this subsonic climb phase the FSPT algorithm was modified by limiting the value of γ^c between -1° and +21°. This modification reduced the errors in all the vertical examples (1-3) by approximately 0.5 sec. The origin of the main part of the remaining error is most probably in the zoom phase. The FSPT algorithm predicts a quasi-constant specific energy zoom[12] with a load factor of the order of 2 while in the optimal solution this value is of the order of 1.5-1.6. The final result seems to be, even with the long zoom of Example No. 3, very satisfactory.

The first step in the analysis of the coupling between horizontal and vertical turning dynamics is to compare the flight path time histories of the optimal solution (MSA) between examples 2 and 5. As seen in Fig. 4 the difference is rather minor. In the 3-D interception (Ex. 5) the aircraft starts with a small dive (loosing no more than 5 m) altitude which is compensated by a slightly higher maximum flight path angle (19.8° instead of 18.25°) at M=0.94, where the transonic phase starts. The reason for

Table 4. Interception time [sec]

Example No.	1	2	3	4	5	6
Open-loop Optimal (MSA)	122.78	124.03	113.99	139.85	138.26	135.12
DDP/CCP Updating	122.90	124.35	114.67	140.91	138.84	135.83
FSPT (original)	123.56	124.86	115.02	141.49	139.61	136.24
FSPT (modified)	122.88	124.24	114.54	140.09	138.49	135.54

this dive is that in the initial specific energy level and at the given required turning rate the optimal speed for acceleration is about 270 m/sec reached at the end of the diving phase (t=4.5sec). The effect of this small dive on the optimal performance index is most probably negligible.

This assertion seems to be confirmed by the FSPT approximation, which decouples the optimization of the horizontal and vertical turning boundary layers. The three-dimensional "original" version is based on a non-modified vertical algorithm[12] and a horizontal algorithm based on a single reduced-order direction χ^R updating. This algorithm provides a pay-off error of the order of 1% which is still marginally satisfactory. A combination of an improved horizontal updating process, - which takes into account the zoom-phase also and consequently predicts with good accuracy the optimal value of χ^R, - as well as the already used limitations imposed on γ^C, leads to the "modified" FSPT result which is as accurate as in the vertical cases. Even in examples 4 and 6, where characteristics of respective low-speed and high-speed "yo-yo" maneuvers seem to appear, the decoupled FSPT algorithm does not lose its accuracy.

In all cases the accuracy of the modified FSPT approximation is similar and slightly better than of the updating DDP/CCP. It does not exceed in many cases the relative pay-off error of 0.35% .

VIII. Conclusions

In this paper two feedback approximations were compared to the open-loop optimal solution of minimum-time air-to-air interception problems. The comparison shows that, although the optimal and sub-optimal trajectories are different, the pay-off accuracy of both closed-loop algorithms is very satisfactory.

Both closed-loop algorithms have a clear potential for real-time airborne implementation. Their relative merits can be compared only qualitatively, because each algorithm was implemented on a different computer using different codes. It has to be kept in mind that the DDP/CCP version is essentially a fast updating of an open-loop algorithm and therefore sensitive to the selection of nominal control. The FSPT algorithm is basically in an explicit feedback form, but it requires some iterative computations for improving its accuracy. Such iterative (updating) computations can be carried out in parallel with the feedback control computations and therefore have no effect on the real-time potential. It seems therefore that an eventual combination of the DDP and FSPT algorithms can be a very successful compromise. This topic requires, however, a more thorough future investigation.

References

1. Kelley, H.J., "Aircraft Maneuver Optimization by Reduced Order Approximation", in Control & Dynamic Systems. Vol. 10, Leondes, C.T. (ed.), Academic Press, 1973, pp. 131-178.

2. Calise, A.J., "Singular Perturbation Methods for Variational Problems in Aircrafts Flight", IEEE Trans. on Automatic Control, Vol. AC-21, 1976, pp. 345-353.

3. Ardema, M.K., "Solution of the Minimum Time to a Climb Problem by Matched Asymptotic Expansions", AIAA J., Vol. 14, No. 7, 1976, pp. 843-850.

4. Mehra, et al., "A Study of the Applications of Singular Perturbation Theory", NASA CR-3167, 1979.

5. Shinar, J. and Merari, A., "Aircraft Performance Optimization by Forced Singular Perturbation", 12th ICAS Congress, Münich, Germany, Oct. 1980.

6. Negrin, M. and Shinar, J., "Solution of Three-Dimensional Interception by In clined Plane Using the Forced Singular Perturbations Technique", 24th Israel Annual Conference on Aviation and Astronautics, Feb. 1982.

7. Calise, A.J. and Moerder, D.D., "Singular Perturbation Techniques for Real-Time Aircraft Trajectory Optimization and Control", NASA CR-3597, 1982.

8. Shinar, J. and Negrin, M., "An Explicit Feedback Approximation for Medium Range Interceptions in the Vertical Plane", Optimal Control Applications and Methods, Vol. 4, No. 4, 1983, pp. 303-323.

9. Shinar, J., "Development of Advanced Guidance Laws for Air Combat", TAE Report No. 555, Sept. 1984.

10. Huynh, H.T. and Moreigne, D., "Quasi-Optimal On-Line Guidance Laws for Military Aircraft", AIAA Paper No. 85-1977-CP, Guidance and Control Conference, Snowmass, Co. 1985.

11. Visser, H.G. and Shinar, J., "A Highly Accurate Feedback Approximation for Variable Speed Interceptions in the Horizontal Plane", AIAA Paper No. 85-1783-CP, 12th Atmospheric Flight Mechanics Conference, Snowmass, Co. 1985.

12. Shinar, J. and Feinstein, V., "Improved Feedback Algorithms for Optimal Maneuver in the Vertical Plane", AIAA Paper No. 85-1976-CP, Guidance and Control Conference, Snowmass, Co. 1985.

13. Price, D.B., Calise, A.J. and Moerder, D.D., "Piloted Simulation of an Algorithm for Onboard Control of Time-Optimal Intercept", NASA TP-2445, 1985.

14. Jones, F.P., Duke, E.L. and Calise, A.J., "Flight Test Experience from a Three-Dimensional Optimal Interception of a Maneuvering Target", Second Int. Symp. on Differential Game Applications, Williamsburg, Va. August 1986.

15. Shinar, J., Negrin, M., Well, K.H., Berger, E., "Comparison Between the Exact and an Approximate Feedback Solution for Medium Range Interception Problems", Invited paper for the 1981 Joint Automatic Control Conf., Charlottesville Virginia, June 1981.

16. Järmark, B., "Convergence Control in Differential Dynamic Programming Applied to Air-to-Air Combat", AIAA J., Vol. 14, No. 1, pp. 118-121, 1976.

17. Stoer, J., Bulirsch, R., "Introduction to Numerical Analysis", Springer Verlag, New York, Heidelberg, Berlin, 1980.

18. Grimm, W., Oberle, H.J., Berger, E., "User Guide for BNDSCO (Boundary Solution)", DFVLR-Mitteilung 85-05, (in German), 1985.

19. Well, K.H., Berger, E., "Minimum Time 180 Deg. Turns of Aircraft", Journal of Optimization Theory and Applications, Vol. 38, No. 1, Sept. 1982.

20. Jacobson, D.H. and Mayne, D.Q., "Differential Dynamic Programming", Elsevier, New York, 1970.

21. Järmark, B., "Differential Dynamic Programming Techniques in Differential Games", in Control and Dynamic Systems, Vol. 17, Leondes, C.T. (ed.), Academic Press, New York, 1981.

22. Anderson, G.M., "Feedback Control for Pursuit-Evasion Problems Between Two Spacecraft Based on Differential Dynamic Programming", AIAA 15th Aerospace Science Meeting, Los Angeles, January 24-26, 1977.

23. Järmark, B., "Near-Optimal Closed-Loop Strategy for Aerial Combat Games", Report TRITA-REG-7602, The Royal Institute of Technology, Dept. of Automatic Control, Stockholm, Sweden, March 1976.

24. Järmark, "On Closed-Loop Controls in Pursuit-Evasion", J. of Computers and Mathematics with Applications (special issue on Pursuit-Evasion Differential Game), To be published 1986.

25. Järmark, B., "Closed-Loop Controls for Pursuit-Evasion Problems Between Two Aircraft", 2nd Int. Symp. on Differential Game Applications, Williamsburg, Virginia, August 21-22, 1986.

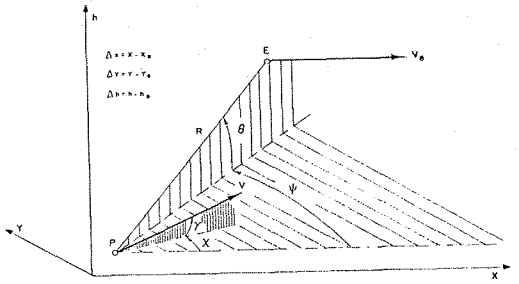

Fig. 1: Geometry of three-dimensional interception.

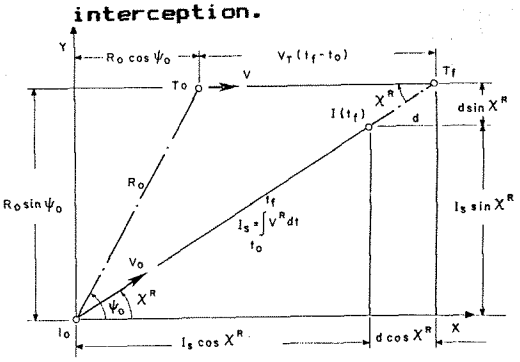

Fig. 2: Horizontal projecton of the reduced-order solution.

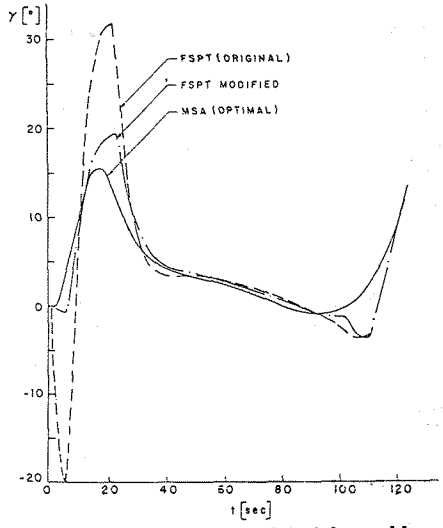

Fig. 3: Comparison of flight path angle time histories (Example 1).

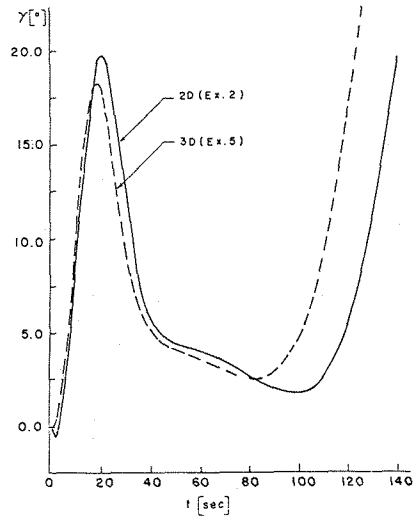

Fig. 4: Comparison of optimal flight path angle time histories (Examples 2 and 5).